Abundance, fatty acid composition and saturation index of neutral lipids are significantly different between isogenic primary and metastatic colon cancer cell lines

Rimsha Munir[1,2], Jan Lisec[3], Carsten Jaeger[4, 5] and Nousheen Zaidi[1,2*]

[1]Cancer Biology Lab, MMG, University of the Punjab, Lahore, Pakistan, [1]Cancer Research Centre, University of the Punjab, Lahore, Pakistan, [3]Bundesanstalt für Materialforschung und -prüfung (BAM), Berlin, [4]Charité - Universitätsmedizin Berlin, Molekulares Krebsforschungszentrum (MKFZ), Augustenburger Platz 1, 13353 Berlin, [5] Berlin Institute of Health (BIH), Anna-Louisa-Karsch-Straße 2, 10178 Berlin, Germany.

***Corresponding author**: Nousheen Zaidi

Email: nosheen.mmg@pu.edu.pk, nzzaidi@yahoo.com

Abstract

Lipid droplets, the dynamic organelles that store triglycerides (TG) and cholesterol esters (CE), are highly accumulated in colon cancer cells. This work studies the TG and CE subspecies profile in colon carcinoma cells lines, SW480 derived from primary tumor, and SW620 derived from a metastasis of the same tumor. It was previously reported that the total TG and CE content is dramatically higher in SW620 cells; however, TG and CE subspecies profile has not been investigated in detail. The presented work confirms that total TG and CE content is significantly higher in SW620 cells. Moreover, the FA-composition of TGs is significantly altered in SW620 cells, with significant decrease in the abundance of saturated triglycerides. This resulted in significantly decreased TG saturation index in SW620 cells. The saturation index of CEs was also significantly decreased in SW620 cells. The saturation indices of some other major lipid classes were either similar or only moderately different between SW480 and SW620 cells. We also compared the expression of metabolic genes that may regulate these changes in the lipidomic profiles.

Keywords: Cancer metabolism, colon cancer, fatty acid saturation, lipid droplets, lipidomics, triglycerides.

52 **Introduction**

53 Lipidomic landscape of colorectal cancer (CRC) cells is significantly modified in comparison to that
54 in their non-malignant counterparts (reviewed in [1]). Primary and metastatic colon cancer cells
55 also display differences in their lipidomic profiles [2]. Previous works have taken advantage of
56 SW480/SW620 cell line pair, which represents an accepted model to study metastatic progression
57 [3]. SW480 is derived from a primary tumor, and SW620 is derived from a metastasis of the same
58 tumor [4]. Multiple differences in the lipidomic profiles of these two cell lines have been noted [2].
59 For instance; increased levels of plasmanylcholine, while decreased levels of
60 plasmenylethanolamine, C-16 containing sphingomyelin and ceramide were observed [2]. It has
61 been shown that , SW620 cells display dramatic increase in total triglyceride (TG) and cholesterol
62 ester (CE) levels [2]. However, the TG and CE subspecies profiles has not been explored in detail.
63 Studying the TG and CE profile CRC cells is particularly important because these neutral lipids from
64 hydrophobic core of lipid droplets (LDs) –that are highly accumulated in CRC cells [5]. Previous
65 works have shown that exposure to excessive poly unsaturated fatty acids (PUFAs) induces LD
66 formation in both SW480 and SW620 cells [6]. Interestingly, SW620 cells accumulate PUFA-
67 enriched CEs, while SW480 cells accumulates PUFA-enriched TGs [6]. This indicates differential
68 regulation of TG and CE content in SW480 and SW620 cells. Herein, we study the differences in TG-
69 and CE-subspecies profiles and saturation index (SI) between SW480 and SW620 cells. Moreover,
70 the expression of various metabolic genes that may bring about these lipidomic changes were also
71 analyzed.

72

73

74

75

76 **Materials and Methods**

77 **Cell culture**

78 The SW480 and SW620, cell lines were purchased from American Type Culture Collection and were
79 maintained in DMEM (Gibco, 31966-021) supplemented with 10% fetal bovine serum (FBS) (Sigma,
80 F75240) and penicillin-streptomycin solution (Corning, 30-002-CI). Cell cultures were maintained
81 in the atmosphere of 5% CO_2 and 37°C. Cell lines were commercially authenticated (Eurofins,
82 Germany) and mycoplasma tested prior to submission of this manuscript.

83 **Gene Expression Analysis**

84 For quantitative RT-PCR, total RNA was extracted from cell pellets using Quick-RNA™ MiniPrep Plus
85 (Zymo Research). All RNA samples were reverse-transcribed into cDNA using SuperScript™ III
86 Reverse Transcriptase (Thermo Scientific, 18080093) and Oligo(dT)18 Primers (Thermo Scientific,
87 SO131). Quantitative PCR was performed using a TaqMan™ Gene Expression Master Mix (4369016,
88 Applied Biosystems) *via* StepOne Real-Time PCR Systems (Applied Biosystems). The TaqMan Gene
89 Expression assays used were Hs01005622_m1 (fatty acid synthase, FASN), Hs00168352_m1 (3-
90 hydroxy-3-methylglutaryl-CoA reductase, HMGCR), Hs00996004_m1 (monoglyceride lipase,
91 MGLL), Hs00173425_m1 (lipoprotein lipase, LPL) and Hs00354519_m1 (CD36). The expression of
92 each gene was normalized to the expression of GADPH (Hs02786624_g1). Microarray data were
93 obtained from publicly accessible gene expression profile database GEO
94 (http://www.ncbi.nlm.nih.gov/geo/). Provenzani *et al* [7] performed a microarray study, analyzing
95 differential gene expression in SW480 and SW620 cells (data accessible at NCBI GEO database,
96 accession GSE2509)

97 **Lipid Extractions**

98 First, the cell pellets were washed with 0.5 mL 0.9% NaCl. For extraction of lipids the pellets were
99 resuspended in 1 ml ice-cold MMC (1:1:1 v/v/v methanol/MTBE/chloroform). Samples were

100 incubated on an ultrasonic bath for two minutes. Phase separation was induced by adding 300 µL
101 MS-grade water. After 10 min incubation, the samples were centrifuged for 10 min at 1000 rpm and
102 the upper (organic) phase was collected. Then 200 µL of collected organic phase were dried in a
103 vacuum rotator and stored at –20 °C until analysis.

104 **Determination of Total Triglyceride and Cholesterol Ester Contents**

105 Total triglyceride content in the lipid extracts was spectrophotometrically determined using
106 commercially available kit (Analyticon Biotechnologies AG, Catalogue # 5052) against a calibration-
107 curve generated using known concentrations of triglyceride standard (SUPELCO, 17811-1AMP).
108 Cholesteryl esters were quantified using Cholesterol/ Cholesteryl Ester Quantitation Kit (Abcam,
109 ab65359) was used according to manufacturer's guidelines.

110 **Lipidomic Profiling and Data Analysis**

111 Dried sample extracts were reconstituted in 100 µL 2:1:1 v/v/v isopropanol/acetonitrile/water. 5
112 µL aliquots were injected into an ACQUITY I-class ultra-performance liquid chromatography
113 (UPLC) system (Waters, Germany) coupled to an Impact II high-resolution quadrupole time-of-
114 flight mass spectrometer (Bruker Daltonik GmbH, Germany). Chromatographic separation was
115 achieved by gradient elution (%A: 0 min, 60; 1.2 min, 57; 1.26 min, 50; 7.2 min, 46; 7.26 min, 30;
116 10.8 min, 0; 12.96 min, 0; 13.02 min, 60; 14.4 min, 60) using a buffered solvent system (A: 60:40
117 v/v acetonitrile/water, B: 90:10 v/v isopropanol:water, both with 10 mM ammonium formate and
118 0.1% formic acid) and a 2.1 mm × 75 mm × 1.7 µm CSH-C18 column (Waters, Germany) equipped
119 with an 0.2 µm pre-column in-line filter. The flow rate was 0.5 mL min-1 and column temperature
120 was 55°C. Electrospray ionization (ESI) conditions were as follows: polarity (+), capillary voltage,
121 4500 V, end plate offset, 500 V, nebulizer pressure, 2.5 bar, dry gas (N2) flow, 8 L/min. Ion transfer
122 parameters were set to: Funnel 1 RF, 200 Vpp, Funnel 2 RF, 200 Vpp, Hexapole RF, 50 Vpp,
123 Quadrupole Ion Energy, 5 eV, Low Mass, 100 m/z, Collision Energy, 8.0 eV, Pre Pulse Storage, 6.0 µs,

124 Stepping Mode, Basic, Collision RF, 500-1000 Vpp, Transfer Time, 60-100 μs, Timing, 50/50,
125 Collision Energy, 100-250%. Alternating MS and MS/MS scans were acquired using a Sequential
126 Windowed Acquisition of All Theoretical Fragment Ion Mass Spectra (SWATH) scheme (m/z 350-
127 975, width 25 Da). For internal calibration, Na formate clusters were spiked into the LC effluent at
128 the end of each run. After data acquisition, files were converted to Analysis Base File (ABF) format
129 using a publicly available converter (Reifycs, Japan) and imported into MS-DIAL (Tsugawa et al.
130 2015). MS-DIAL parameter settings were as follows: Soft Ionization, Data independent MS/MS,
131 Centroid data, Positive ion mode, Lipidomics. Detailed analysis settings were left at default, except
132 for Retention time end (10 min), Alignment Retention time tolerance (0.2 min), Identification
133 Retention time tolerance (3 min) and Identification score cut off (60%).

134 For each of 6 replicate samples per cell line we calculated within each major lipid class the relative
135 distribution of lipids containing none (SFA0), exactly one (SFA1) and two or more saturated fatty
136 acids (SFA2). To this end, the measured ion intensities for the groups (SFA0, 1 and 2) were summed
137 up and normalized to the total sum of this lipid class. Mean values and standard deviations for the
138 SFA distribution were calculated over the 6 replicates per cell line. Saturation indices were
139 calculated as a ratio of total saturated fatty acid content to total unsaturated fatty acid content [8]
140 within each major lipid class. Total content of saturated fatty acids was calculated by summing up
141 the intensities of all lipids multiplied by the number of saturated fatty acids present within each
142 lipid. Total content of un-saturated fatty acids in each individual lipid class was calculated by
143 summing up the intensities of all lipids multiplied by the number of un-saturated fatty acids present
144 within each lipid. To compare SI over lipid classes we normalized with respect to the SI value
145 obtained for SW480.

146 **Statistical analysis**

147 The differences between groups were analyzed by ANOVA or t-test (paired or unpaired), where
148 applicable. Statistical analyses and graphical representations for lipidomic data and quantitative

149 RT-PCR data were performed using the R software environment 3.4.2 (http://cran.r-project.org/)
150 or MetaboAnalyst 3.5 (http://www.metaboanalyst.ca/faces/home.xhtml). P-values <0.05 were
151 considered statistically significant and indicated when different.

152 **Results and Discussion**

153 A previous study has shown a dramatic increase in abundance of total cholesterol esters (CEs) and
154 triglycerides (TGs) in SW620 cells in comparison to SW480 cells [2]. We also assessed the total TG
155 and CE content and observed that SW620 cells display 2.5-3 fold increase in the levels these storage
156 lipids (**supplementary figure 1**). Next, the fatty acid (FA) composition of TGs and CEs was
157 compared. We observed that in SW480 cells the triglycerides (TGs) with ≥2 saturated fatty acids
158 (SFA) were in the highest proportion (i.e. 61%). The proportion of TGs containing 1 or 0 SFA was
159 35% and 4%, respectively. These proportions were significantly altered in SW620 cells in which the
160 proportion of TGs with ≥2 saturated fatty acids was decreased to 40%, while the proportions of TGs
161 containing 1 or 0 SFA were respectively increased to 53% and 7%. In agreement to these results,
162 the TG saturation index (SI) was markedly higher in SW480 cells than in SW620 cells. On the other
163 hand, FA-composition and SI of diacylglycerols (DGs), the direct precursors to TGs, was only slightly
164 altered. The FA-composition of CEs also showed minor changes, with slight shift in the proportions
165 of CEs containing 0 or 1 SFA. However, the SI of CEs was also significantly decreased in SW620 cells.
166 We also compared the FA composition of the most abundant membrane lipids,
167 phosphatidylcholines (PCs) and phosphatidylethanolamine (PEs), in SW480 and SW620 cells. No
168 substantial differences were observed in fatty acid composition and SI of PCs and PEs (**Figure 1**).
169 Hence, TGs constitute the major lipid class that displays changes in FA composition in SW620 cells
170 when compared to SW480 cells.

171 To understand the molecular mechanisms regulating these changes in the lipidomic profiles, we
172 performed expression analyses and also used publicly accessible gene expression profile database

173 GEO (http://www.ncbi.nlm.nih.gov/geo/). **Figure 2** displays overview of the major cancer-
174 associated lipid metabolism pathways. The fold-changes in the expression levels of various
175 genes/enzymes are indicated with a colored-box on *left-side* of the respective gene symbol. For
176 color-codes see color-key on *top-left* corner of **Figure 2**. As discussed above, the differences in the
177 FA composition of TGs was the most significant difference between lipidomic profiles of SW480 and
178 SW620 cells, with SW620 cells displaying significantly lower TG saturation-index. A recent study
179 has shown that gene silencing of diglyceride acyltransferases (DGATs) –enzymes that catalyze
180 formation of TGs from DGs and Acyl CoA– induces increase in TG saturation-index [9]. Hence,
181 increased expression of DGAT might induce decreased SI in TGs. Our analyses revealed that
182 expression of DGAT was slightly decreased (1-1.5 Fold) in SW620 cells (**Figure 2, TG Synthesis**).
183 Hence, DGAT expression might not be responsible for the changes in TG saturation-index of SW620
184 cells.

185 Next, we looked at other lipid metabolism pathways that have been implicated in regulation of lipid
186 saturation-indices. Highly active *de novo* FA synthesis induces increased SFAs or MUFAs levels in
187 cancer cell cells [10]. The expression of FA synthesis genes is up-regulated in SW620 cells, hence
188 this pathway is also not contributing in decreased SI in these cells (**Figure 2, FA Synthesis**).

189 Major genes of intracellular lipolytic pathway –including PNPLA2, HSL and MGLL– are all down
190 regulated in SW620 cells (**Figure 2, Intracellular Lipolysis**). This may explain the dramatic
191 increase in total triglyceride (TG) levels in SW620 cells. However, specific decrease in ≥2 SFA
192 containing TGs could not be explained by this mechanism.

193 The expression of ACADM and ACADL –the enzymes that catalyze the first step of FA oxidation in
194 mitochondria– is differentially regulated in SW620 cells. The expression of ACADM was up
195 regulated, while the expression of ACADL was down-regulated in SW620 in comparison to SW480
196 cells (**Figure 2, FA Oxidation**). This observation is of special interest in this context, because

197 ACADL is known to mediate unsaturated FA oxidation, whereas ACDM prefers saturated FAs as
198 substrates. Hence, it is possible that in SW620 cells there is an increased oxidation of SFAs, while
199 decreased oxidation of unsaturated FAs. This may cause selective depletion of SFAs in the stored
200 lipids and induced decreased SI of TGs and CEs. Recent studies have shown that disruptions in lipid
201 metabolism or nutrient/oxygen supply also drastically affects FA-composition of TGs in cancer
202 cells, while the FA-composition of other lipid classes is not significantly affected [9,11]. Hence, FA-
203 composition of TGs is most markedly affected by the changes in cancer stage, tumor
204 microenvironment and de novo FA synthesis. Further studies are required to understand the
205 significance of fatty acid composition of TGs in cancer progression and survival.

206

207

208

209

210

211

212

213

214

215

216

217

218

219 **Abbreviations**

220 FASN, fatty acid synthase; HMGCR, 3-hydroxy-3-methylglutaryl-CoA reductase; MGLL,
221 monoacylglycerol lipase; LPL, lipoprotein lipase; PC, Phosphatidylcholines; PE,
222 Phosphatidylethanolamines; PPE, Plasmenylphosphatidylethanolamines; PPC,
223 Plasmenylphosphatidylcholines; TG, Triacylglycerols; CE, Cholesterol esters and DG,
224 Diacylglycerols.

225 **Declarations**

226 **Ethics approval and consent to participate**

227 Not applicable.

228 **Consent for publication**

229 Not applicable.

230 **Availability of Data and Material**

231 The datasets supporting the conclusions of this article are included within the article and
232 supplementary files.

233 **Competing Interests**

234 The authors declare no potential competing interests.

235 **Funding**

236 This work was financially supported by Alexander von Humboldt Foundation (Georg Forster
237 Research Fellowship for Experienced Researchers awarded to N. Zaidi) and University of the
238 Punjab under Projects for Cancer research Centre (PI: N. Zaidi). Funding bodies did not play any
239 role in study designing; data collection, analysis, & interpretation or manuscript writing.

240 **Acknowledgments**

241 We are grateful to Mr. Banaras Masih for his technical assistance for this project.

242

243

244

Authors' Contributions

This study was designed by NZ. Experimental work was done by NZ, CJ and RM; and data was analyzed and interpreted by JL, CJ, NZ and RM. The manuscript was written by RM and NZ; and reviewed and approved by all authors.

References

[1] A. Pakiet, J. Kobiela, P. Stepnowski, T. Sledzinski, A. Mika, Changes in lipids composition and metabolism in colorectal cancer: a review, Lipids Health Dis 18 (2019) 29.

[2] C.J. Fhaner, S. Liu, H. Ji, R.J. Simpson, G.E. Reid, Comprehensive lipidome profiling of isogenic primary and metastatic colon adenocarcinoma cell lines, Anal Chem 84 (2012) 8917-8926.

[3] R.E. Hewitt, A. McMarlin, D. Kleiner, R. Wersto, P. Martin, M. Tsokos, G.W. Stamp, W.G. Stetler-Stevenson, Validation of a model of colon cancer progression, J Pathol 192 (2000) 446-454.

[4] A. Leibovitz, J.C. Stinson, W.B. McCombs, 3rd, C.E. McCoy, K.C. Mazur, N.D. Mabry, Classification of human colorectal adenocarcinoma cell lines, Cancer Res 36 (1976) 4562-4569.

[5] L. Tirinato, C. Liberale, S. Di Franco, P. Candeloro, A. Benfante, R. La Rocca, L. Potze, R. Marotta, R. Ruffilli, V.P. Rajamanickam, M. Malerba, F. De Angelis, A. Falqui, E. Carbone, M. Todaro, J.P. Medema, G. Stassi, E. Di Fabrizio, Lipid droplets: a new player in colorectal cancer stem cells unveiled by spectroscopic imaging, Stem Cells 33 (2015) 35-44.

[6] S.A. Schonberg, A.G. Lundemo, T. Fladvad, K. Holmgren, H. Bremseth, A. Nilsen, O. Gederaas, K.E. Tvedt, K.W. Egeberg, H.E. Krokan, Closely related colon cancer cell lines display different sensitivity to polyunsaturated fatty acids, accumulate different lipid classes and downregulate sterol regulatory element-binding protein 1, Febs j 273 (2006) 2749-2765.

[7] A. Provenzani, R. Fronza, F. Loreni, A. Pascale, M. Amadio, A. Quattrone, Global alterations in mRNA polysomal recruitment in a cell model of colorectal cancer progression to metastasis, Carcinogenesis 27 (2006) 1323-1333.

[8] D. Ackerman, S. Tumanov, B. Qiu, E. Michalopoulou, M. Spata, A. Azzam, H. Xie, M.C. Simon, J.J. Kamphorst, Triglycerides Promote Lipid Homeostasis during Hypoxic Stress by Balancing Fatty Acid Saturation, Cell Rep 24 (2018) 2596-2605.e2595.

[9] D. Ackerman, S. Tumanov, B. Qiu, E. Michalopoulou, M. Spata, A. Azzam, H. Xie, M.C. Simon, J.J. Kamphorst, Triglycerides Promote Lipid Homeostasis during Hypoxic Stress by Balancing Fatty Acid Saturation, Cell reports 24 (2018) 2596-2605. e2595.

[10] E. Rysman, K. Brusselmans, K. Scheys, L. Timmermans, R. Derua, S. Munck, P.P. Van Veldhoven, D. Waltregny, V.W. Daniëls, J. Machiels, De novo lipogenesis protects cancer cells from free radicals and chemotherapeutics by promoting membrane lipid saturation, Cancer research (2010) 0008-5472. CAN-0009-3871.

[11] J. Lisec, C. Jaeger, R. Rashid, R. Munir, N. Zaidi, Cancer cell lipid class homeostasis is altered under nutrient-deprivation but stable under hypoxia, BMC Cancer 19 (2019) 501.

307 **Figure Legends**

308 **Figure 1: Comparison of fatty acid composition and saturation indices in major lipid classes**
309 **in SW480 and SW620 cells.** The figure is structured in five rows and three columns. Rows show
310 data for the major lipid classes Triglycerides (TG), Diglycerides (DG), Cholesterol Esters (CE),
311 Phosphatidylethanolamines (PE) and Phosphatidylcholines (PC), Left column displays lipid class ID
312 and a legend indicating the number of lipid-subspecies within each lipid class containing different
313 numbers of saturated fatty acids (0, 1 or ≥2SFAs). Center column shows the relative amount (in per
314 cent of summed ion intensity) of lipid subspecies within both SW cell lines. Numeric values for
315 mean and standard deviation calculated over 6 replicate samples per cell line are given within the
316 bars. Right column displays the saturation indices (cf. Method section) of the respective lipid class
317 normalized to SW480.

318 **Figure 2: Fold-changes in expression levels of various genes in major lipid metabolism**
319 **pathways in SW620 *vs.* SW480 cells.** The figure highlights all the key lipid metabolism pathways
320 activated in cancer cells. Major pathways are shown as boxes without outlines. The systematic
321 names of these pathways are given in each box. The fold-changes in the expression levels of various
322 genes/enzymes in SW620 cells compared with SW480 cells are indicated with a colored-box on *left-*
323 *side* of the respective gene symbol. For color-codes see color-key on *top-left* corner. The expression
324 data for these analyses were extracted from at NCBI GEO database, accession GSE2509. For some
325 markers gene expression analysis was performed (**Supplementary Figure S2**). The symbols within
326 fold-change boxes represent the data source (G; GEO database, S, Supplementary Figure S2).
327 **Abbreviations:** ACACA, acetyl-CoA carboxylase 1; ACACB, acetyl-CoA carboxylase 2; ACSS2, acyl
328 Co-A synthetase-2; ADFP, adipose differentiation protein; ATGL, adipose triglyceride lipase; FA,
329 fatty acids; FABP3, fatty acid binding protein 3; FABP7, fatty acid binding protein 7; FFA, free fatty
330 acids; FASN, fatty acid synthase; H, hypoxia; HIF-1α, hypoxia-inducible factor 1-alpha; HIF-2α,
331 hypoxia-inducible factor 2α; HIG2, hypoxia-inducible gene 2 protein; HMGCR, 3-hydroxy-3-

332 methylglutaryl-CoA reductase; LD, lipid droplet; LCAD, long-Chain Specific acyl-CoA
333 dehydrogenase; MAG, monoacylglycerol ; MCAD, Medium-chain acyl-CoA dehydrogenase; MUFA,
334 monounsaturated fatty acids; PBMCs, peripheral blood mononuclear cells; PC,
335 Phosphatidylcholines; PE, phosphatidylethanolamines; Pcho, propargyl-choline; PI,
336 phosphatidylinositol; PS, phosphatidylserine; PUFA, polyunsaturated fatty acids; SCD, stearoyl-CoA
337 Desaturase; SFA, saturated fatty acids; SREBP, sterol regulatory element-binding proteins; TG,
338 triglycerides.

339

340

341

342

343

344

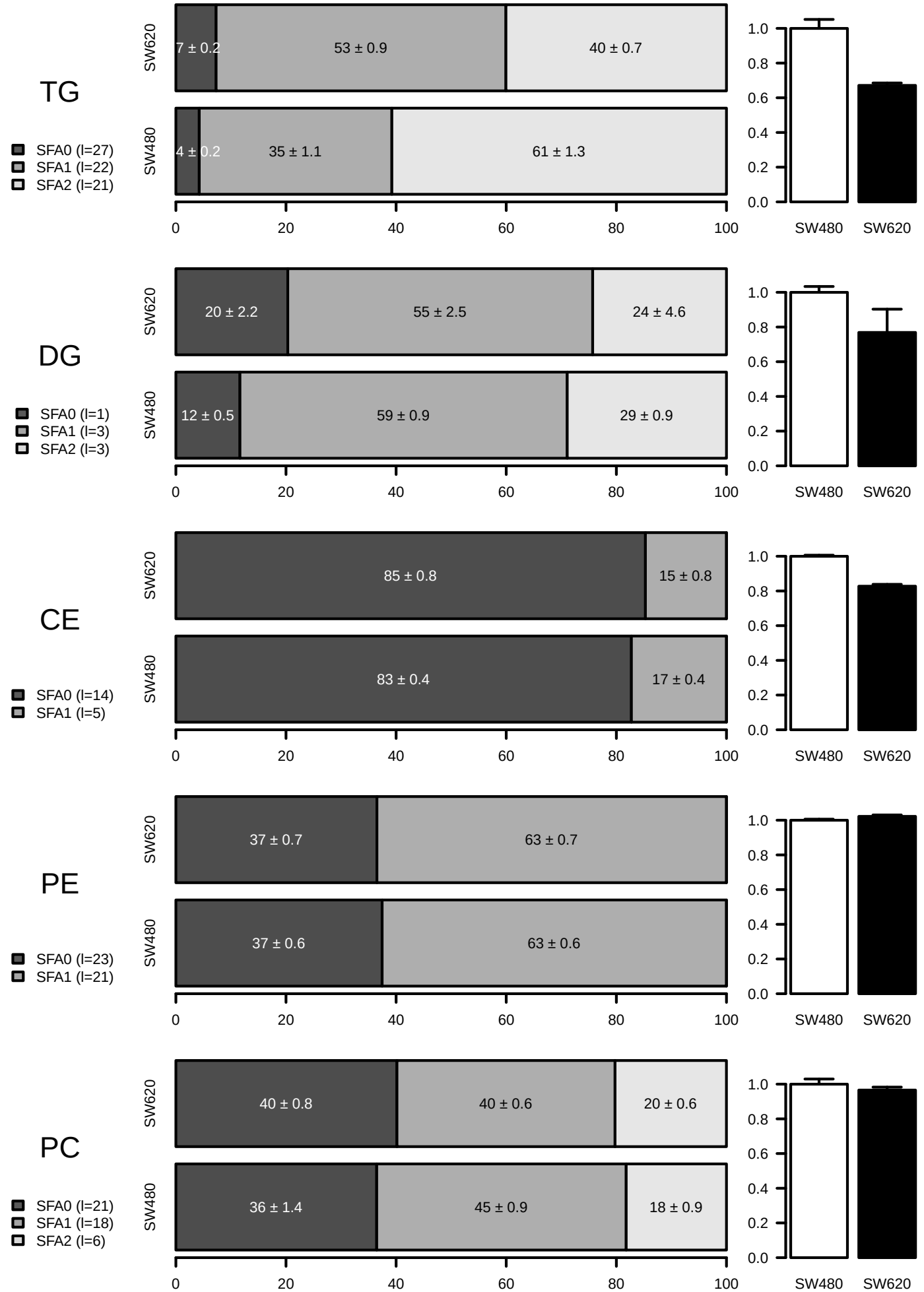
TG
SFA0 (l=27)
SFA1 (l=22)
SFA2 (l=21)
SW620
SW480
7 ± 0.2
53 ± 0.9
40 ± 0.7
4 ± 0.2
35 ± 1.1
61 ± 1.3
DG
SFA0 (l=1)
SFA1 (l=3)
SFA2 (l=3)
20 ± 2.2
55 ± 2.5
24 ± 4.6
12 ± 0.5
59 ± 0.9
29 ± 0.9
CE
SFA0 (l=14)
SFA1 (l=5)
85 ± 0.8
15 ± 0.8
83 ± 0.4
17 ± 0.4
PE
SFA0 (l=23)
SFA1 (l=21)
37 ± 0.7
63 ± 0.7
37 ± 0.6
63 ± 0.6
PC
SFA0 (l=21)
SFA1 (l=18)
SFA2 (l=6)
40 ± 0.8
40 ± 0.6
20 ± 0.6
36 ± 1.4
45 ± 0.9
18 ± 0.9
0
20
40
60
80
100
0.0
0.2
0.4
0.6
0.8
1.0
SW480
SW620

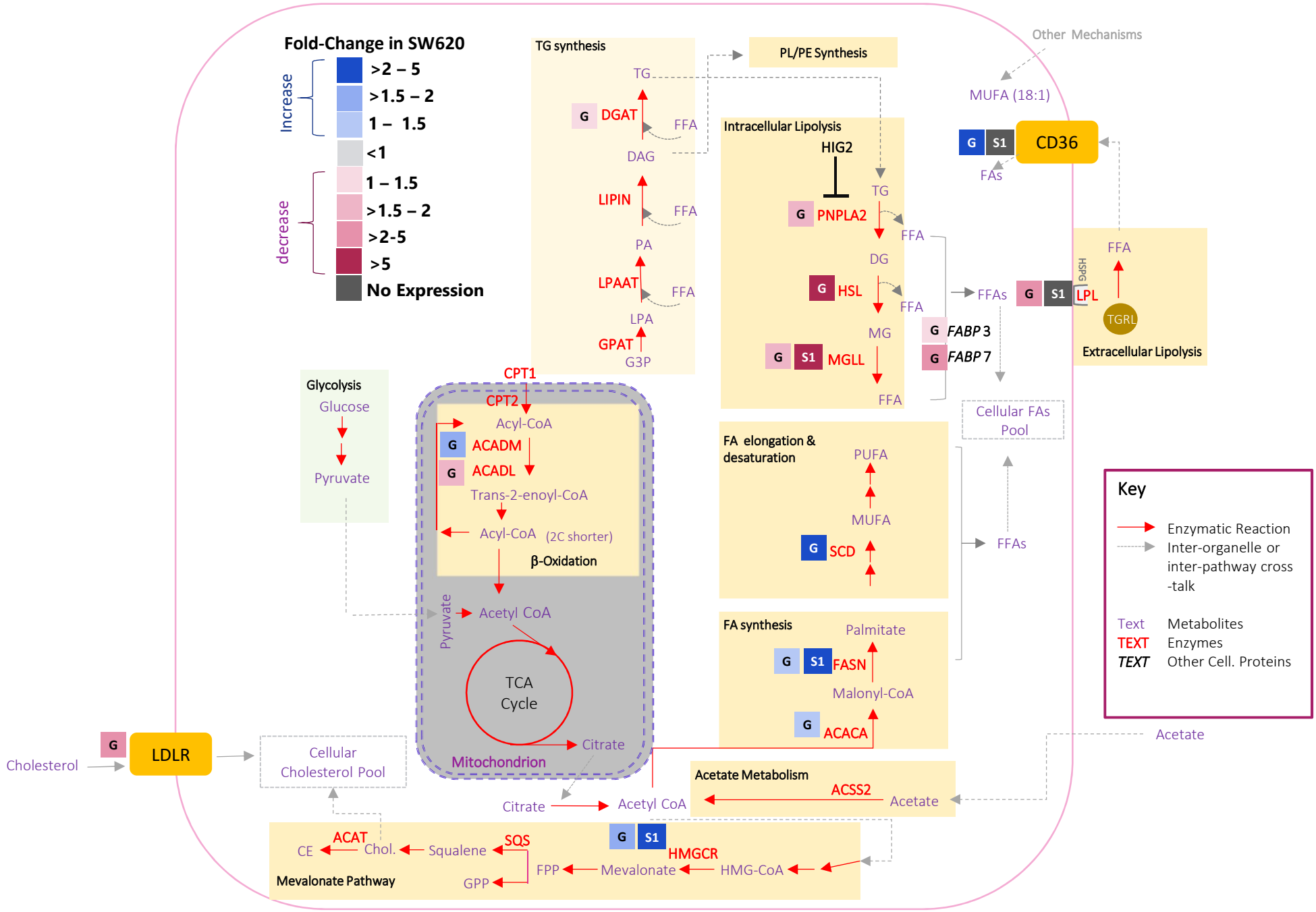
Fold-Change in SW620
Increase
>2 – 5
>1.5 – 2
1 – 1.5
<1
decrease
1 – 1.5
>1.5 – 2
>2-5
>5
No Expression
TG synthesis
TG
G DGAT
FFA
DAG
LIPIN
FFA
PA
LPAAT
FFA
LPA
GPAT
G3P
PL/PE Synthesis
Intracellular Lipolysis
HIG2
TG
G PNPLA2
FFA
DG
G HSL
FFA
MG
G S1 MGLL
FFA
FFAs
G FABP 3
G FABP 7
Other Mechanisms
MUFA (18:1)
G S1 CD36
FAs
FFA
HSPG
G S1 LPL
TGRL
Extracellular Lipolysis
Glycolysis
Glucose
Pyruvate
CPT1
CPT2
Acyl-CoA
G ACADM
G ACADL
Trans-2-enoyl-CoA
Acyl-CoA (2C shorter)
β-Oxidation
Pyruvate
Acetyl CoA
TCA Cycle
Citrate
Mitochondrion
Cellular FAs Pool
FA elongation & desaturation
PUFA
MUFA
G SCD
FFAs
FA synthesis
Palmitate
G S1 FASN
Malonyl-CoA
G ACACA
Key
Enzymatic Reaction
Inter-organelle or inter-pathway cross -talk
Text Metabolites
TEXT Enzymes
TEXT Other Cell. Proteins
Acetate
Cholesterol
G LDLR
Cellular Cholesterol Pool
Citrate
Acetyl CoA
Acetate Metabolism
ACSS2
Acetate
CE
ACAT
Chol.
Squalene
SQS
GPP
FPP
Mevalonate Pathway
G S1 HMGCR
Mevalonate
HMG-CoA

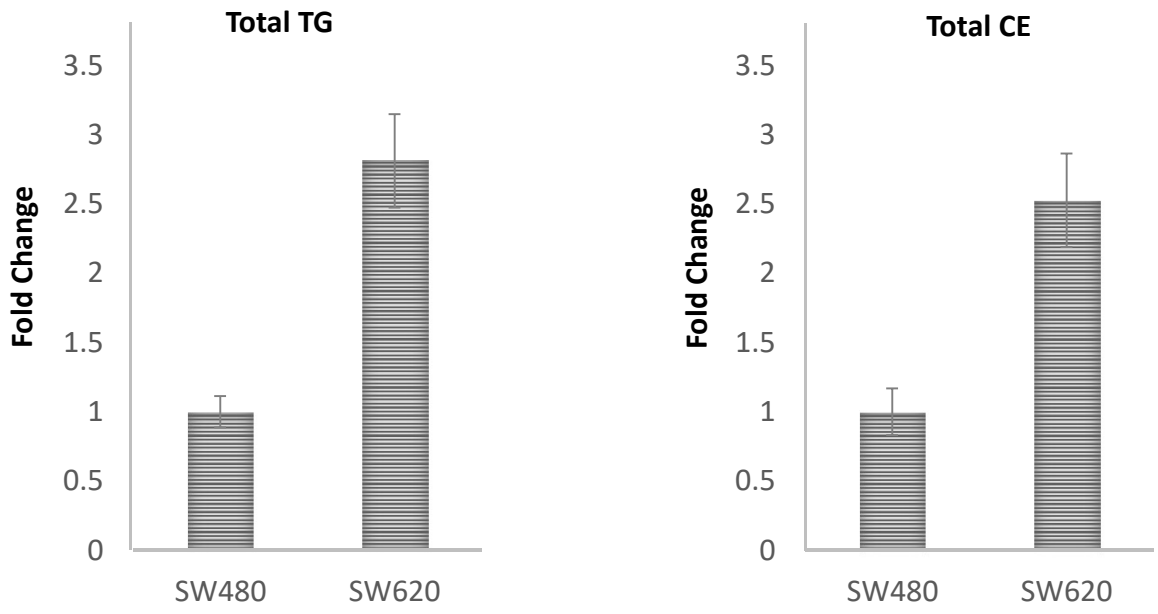

Supplementary Figure S1: Fold-changes in total triglyceride(TG) and cholesterol ester (CE) content in SW480 vs. SW620 cells.

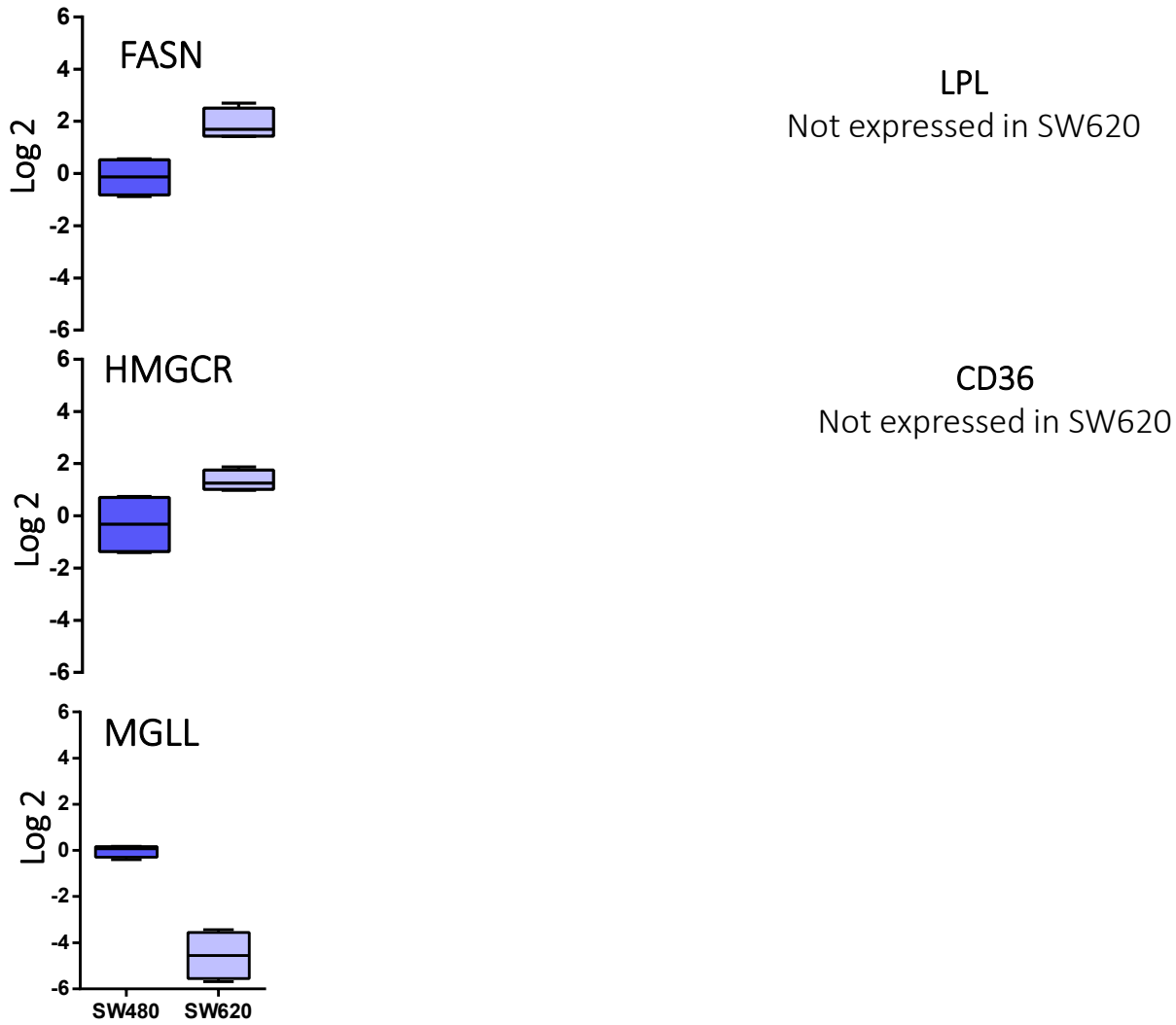

Supplementary Figure S2: Expression of selected genes from de novo lipid synthesis or lipid uptake/degradation pathways in SW480 and SW620 cell lines. Box plots showing log2 transformed and median normalized values of FASN, HMGCR and MGLL. LPL and CD36 expressions were not detected. The levels of the different transcripts were measured in 3 to 6 samples by qPCR. The results show the distribution of corresponding transcripts relative to GAPDH, with the box indicating the 25th–75th percentiles, with the median indicated. line. The whiskers show the range.